Geophysical Journal International

Geophys. J. Int. (2013) doi: 10.1093/gji/ggt160

Geophysical Journal International Advance Access published May 15, 2013

EXPRESS LETTER

Teleseismic correlations of ambient seismic noise for deep global imaging of the Earth

P. Boué, P. Poli, M. Campillo, H. Pedersen, X. Briand and P. Roux

Institut des Sciences de la Terre, Université Joseph Fourier and CNRS, Grenoble, France. E-mail: pierre.boue@ujf-grenoble.fr

Accepted 2013 April 16. Received 2013 April 15; in original form 2013 March 18

SUMMARY

We present here a global analysis showing that wave paths probing the deepest part of the Earth can be obtained from ambient noise records. Correlations of seismic noise recorded at sensors located various distances apart provide new virtual seismograms for paths that are not present in earthquake data. The main arrivals already known for earthquake data are also present in teleseismic correlations sections, including waves that have propagated through the Earth's core. We present examples of applications of such teleseismic correlations to lithospheric imaging, study of the core mantle boundary or of the anisotropy of the inner core.

Key words: Interferometry; Body waves; Wave propagation.

INTRODUCTION

Imaging of the structure of the Earth from its core to the surface is routinely carried out using the energy emitted from earthquakes. However, these techniques suffer from severe limitations, as the major earthquake events are located close to the tectonic plate boundaries. Seismic–noise correlations constitute a valuable supplement (Shapiro & Campillo 2004), although their application has hitherto been limited to the uppermost layers of the Earth, as mainly surface waves that are extracted from the noise. Recently, it was demonstrated that crustal body-wave reflections (Zhan *et al.* 2010; Ruigrok *et al.* 2011; Poli *et al.* 2012a) can be extracted from ambient noise records. Furthermore, coherent deep reflections can also be obtained from correlations within dense regional arrays (Poli *et al.* 2012b; Lin *et al.* 2013). We demonstrate here that at large distances between seismic stations, body waves that have propagated through the entire Earth can not only be extracted from the seismic noise, but also contain sufficient precision to be used for high-resolution imaging techniques in complement to earthquake data. This includes the deepest wave paths that probe the core of the Earth and propagate through its centre.

A permanent seismic signal is produced mainly by interactions between ocean waves and the solid Earth. We refer to this as ambient noise. Indeed, a careful processing is required to remove the contribution from earthquakes, particularly for long-period signals, because reverberations with large duration follow major events, and contribute to the discrete normal mode spectrum.

A component of teleseismic body waves in the noise records is well attested (Vinnik 1973; Gerstoft *et al.* 2008; Landès *et al.* 2010; Nishida 2013). We postulated that because of the low attenuation in the deep Earth, body waves that propagate at depth will bounce repeatedly and will contribute to the surface motion with weak amplitudes, although for long durations. As ballistic waves from large earthquakes can pollute the correlations, we reduced their influence through temporal equalization of the amplitude of the noise records (see supporting information), and additionally, we removed the time windows with the largest earthquakes and storms. In contrast, the late arrivals that arrive after each ballistic wave from earthquakes and large storms, known as the coda waves, are expected to contribute to the correlations, as they have been shown to provide good estimates of the Green's function (Campillo & Paul 2003). Because we look for waves with large apparent velocities, the sources of noise at the surface that contribute coherently to the correlations for given pairs of stations are spread over large regions, which will increase with the number of multiple reflections (Sabra *et al.* 2004).

We here present global body-wave seismograms that were extracted from ambient noise. The existence of the main long-period deep phases in the global correlations was recently shown using a spectral method of filtering based on a spherical normal mode representation that was aimed at improving the signal-to-noise ratio (Nishida 2013). Nishida concluded that the main contribution at long period is the seismic hum, as he designates seismic noise created by oceanic sources. We here carried out further processing that preserved the complexity of the wave propagation in the 3-D heterogeneous Earth without any hypothesis as to symmetries. Our analysis was further extended to periods as low as 5 s, for which the waves contain high-resolution information about the deep Earth structures. We show that the seismograms obtained from the correlations have sufficient precision to be used to image the actual complexity of the Earth.

DATA AND CROSS-CORRELATIONS

We used 1 yr (2008) of vertical records from a set of 339 broadband stations that are distributed globally (Fig. 1a). These included

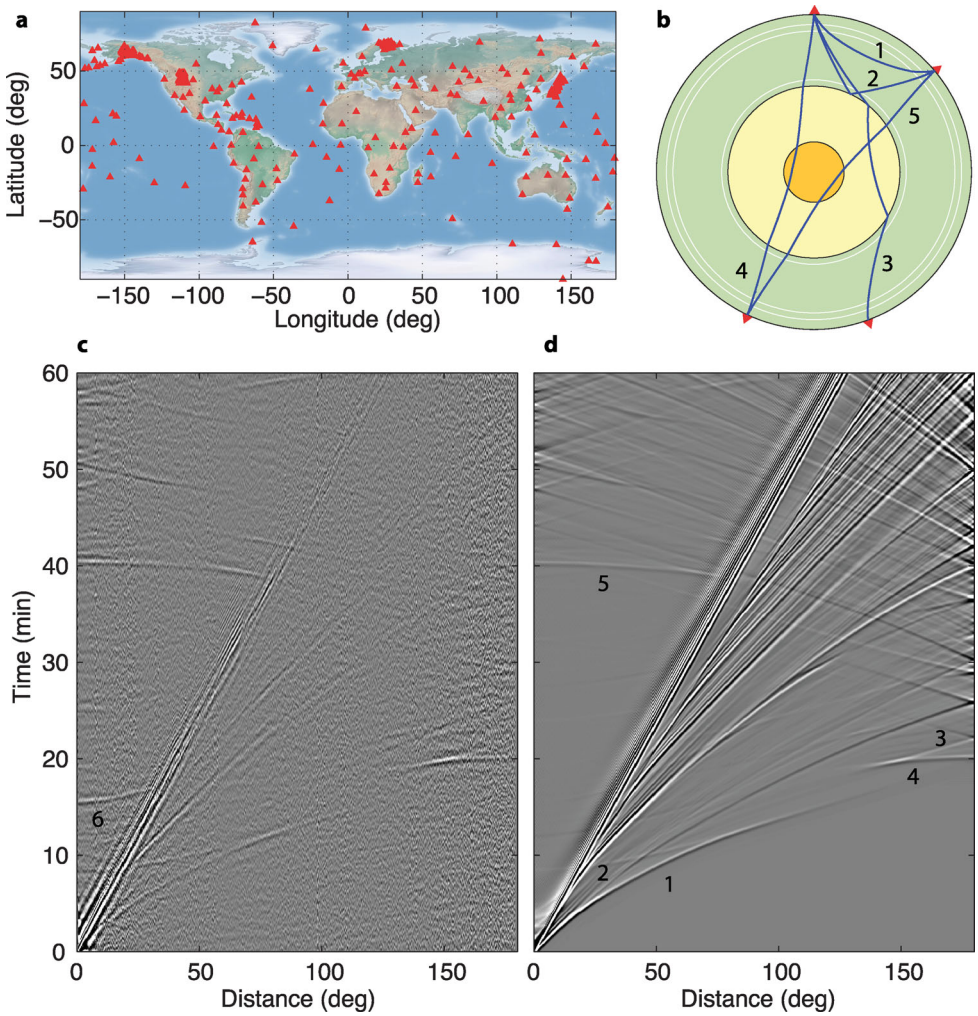

Figure 1. Global seismic section showing the teleseismic body waves from the ambient noise correlations. (a) The locations of the seismic stations used for this study. (b) The global paths of the selected body-wave arrivals (*P* waves: 1, direct [P]; 2, outer-core reflected [PcP]; 3, outer-core passing [PKP]; 4, outer/inner-core passing [PKIKP]; 5, surface-reflected PKIKP plus PKIKP [P′P′]). (c) The raw-noise cross-correlations for the set of stations shown in (a) and filtered in the period band of 25–100 s. The shear wave reflected on the outer core [ScS] is indicated (as 6). (d) The synthetic seismograms for the PREM spherically symmetric earth model. The numbers refer to the paths in (b).

several dense networks that are located in different tectonic regions, some of which had low levels, and others, high levels, of local seismicity. All of the signals were corrected for instrument responses and filtered between 5 and 100 s before the correlation of the data from each of the 57 000 station pairs. The procedure is almost the same as that used for the extraction of mantle reflected body waves (Poli *et al.* 2012b), and it is presented in the supplementary materials. For each individual correlation, the signals in the positive and negative correlation times were stacked to enhance the signal-to-noise ratio.

Fig. 1(c) shows the 1-hr correlations as a function of station-pair distance for the period band of 25–100 s. Note that the distances are shown in degrees, which range up to 180°; that is, the antipode of the stations. For plotting purposes, we stacked the signals by bins of 0.1°. As expected, broad-band noise correlations show clearly dispersive surface (Rayleigh) waves that are the prominent phase at short distances, although numerous other wave arrivals clearly emerge. Fig. 1(d) shows the synthetic seismograms that were computed in the spherical reference PREM (Dziewonski & Anderson 1981) using the spectral element method (Nissen-Meyer *et al.* 2007, 2008). The vertical displacement at each distance was computed for a vertical point-force located at distance 0° and convolved with a Gaussian wavelet of central period 40 s, which corresponds to the maximum in the spectrum of the teleseismic correlations.

We note that the predicted dominant phases (Fig. 1d), such as the P, PP, PcP (see Fig. 1b), S and core phases with the bright spots of PKP triplication and the antipodal reflection PKIKPPKIKP (P′P′df), are easily identified in the correlation sections (Fig. 1c). Other late phases are also visible without further processing (see Fig. S1), such as PKPPKS, PKPPcP, PKiKP, PKIKP, S, SS, SSS, ScS, SKP, SKKP and PcPPKPPKP. In general, the agreement between the noise correlation and synthetics is excellent, especially considering that this correlation section is shown without array processing, which would have increased the apparent signal-to-noise ratio, but which, on the other hand, would have erased the local specificity of each seismogram. The variable wave shape of the Rayleigh waves illustrates the strong heterogeneity of the lithosphere, as the section merges paths across different structures and therefore it produces highly variable dispersion. To a lesser degree, this known heterogeneity of the crust and upper mantle also affects the deep phases and degrades their visual representation, although this complexity is also what we need to explore for imaging purposes.

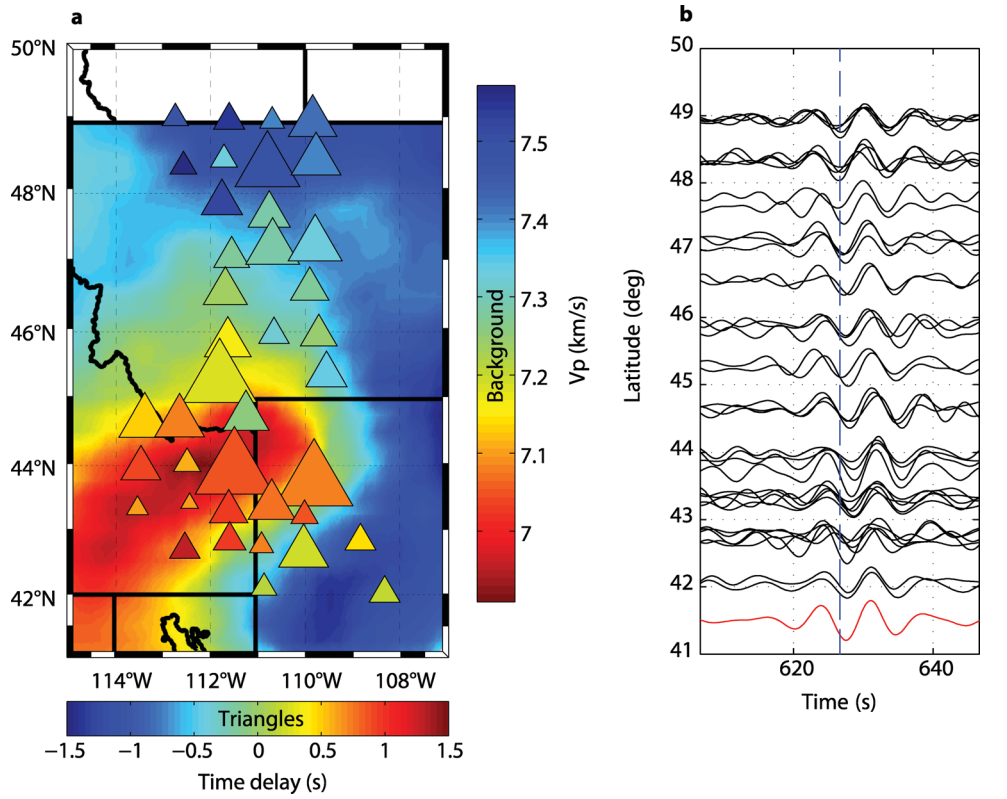

Figure 2. Illustration of the potential use of noise-based traveltime observations for lithospheric tomography. (a) Observed delays of 5–10 s *P* waves at a subset of the USArray stations (triangles; delay colour coded), and a tomographic model (average upper 200 km) of the lithosphere (Shen *et al.* 2013), where we estimated *P* velocities by multiplying *S* velocities by 1.7. The size of each triangle is inversely proportional to the correlation coefficient between reference and measured traces, and represents the quality of the time-delay measurement. (b) Individual station traces (black) and the reference wavelet used to measure time delays (red). The blue line corresponds to the theoretical traveltime at the array centre, used as a reference time.

We also note the presence of a strong ScS phase (shear wave with the same path as the PcP waves, so reflected at the core–mantle boundary; see Fig. 1b) at small epicentral distances, with relative amplitudes much larger than in the theoretical seismograms (the vertical component), for a perfect spherical structure. This strong arrival is not present on the stacks of earthquake records for the vertical component (Astiz *et al.* 1996), with the exclusion of significant conversions close to the receivers. We interpret this discrepancy as a marker of the imperfect reconstruction of the Earth response that is because of an uneven distribution of the noise sources. For elastic vector waves, non-specular contributions produce polarization bias that would disappear with perfect illumination of the receivers (Sánchez-Sesma & Campillo 2006). The high amplitudes of the ScS phase as compared to the *P* waves can be further explained by the dominance of shear wave energy in the long-period noise (Kurrle & Widmer-Schnidrig 2008; Nishida *et al.* 2008). This is in agreement with the model of the generation of seismic shear waves by oceanic infragravity waves (Fukao *et al.* 2010). Another explanation could be that the reverberations of large duration after a large earthquake are only partly removed by standard ambient noise processing. This explanation is favoured by Lin *et al.* (2013) who presented an example of the relationship between earthquake occurrence and amplitude of spurious ScS on vertical components of long-period correlations at short distances. The optimal processing strategies at long periods therefore still needs to be better understood.

In the secondary microseismic period band (5–10 s), in which the ambient noise is predominantly excited by a pressure field at the bottom of the oceans (Longuet-Higgins 1950; Ardhuin *et al.* 2011; Hillers *et al.* 2012), no strong ScS were visible in the teleseismic correlations. Filtered in this band (5–10 s), the cross-correlation section is dominated by *P*-wave arrivals, with clear P, PcP and P′P′ wave paths (see Fig. S2).

To be confident that the body waves extracted from the teleseismic correlations result from the ambient noise and not from contributions of earthquakes that occurred close to one of the stations, we carried out a test in which we selected the data from two seismic networks in regions with completely different seismic activities: LAPNET in Finland, and FNet in Japan. Japan is one of the most seismically active regions, whereas Finland is part of the Archean Baltic shield and is one of the quietest. We separately analysed the correlations for the positive and negative correlation times; that is, the contributions of the waves travelling from Finland to Japan, or from Japan to Finland respectively. In both cases, the P and PcP deep phases are clearly visible, with similar signal-to-noise ratios (see Fig. S3). This indicates that any strong waves from earthquakes in Japan have been correctly removed in our processing, and that their remaining contribution is negligible or consists of a global coda. This test shows that the source of the body-wave signals in the correlations is indeed background ambient noise, rather than ballistic waves from local earthquakes.

POSSIBLE APPLICATIONS

The teleseismic correlations of the ambient noise provided new virtual seismograms that contain information on the heterogeneity

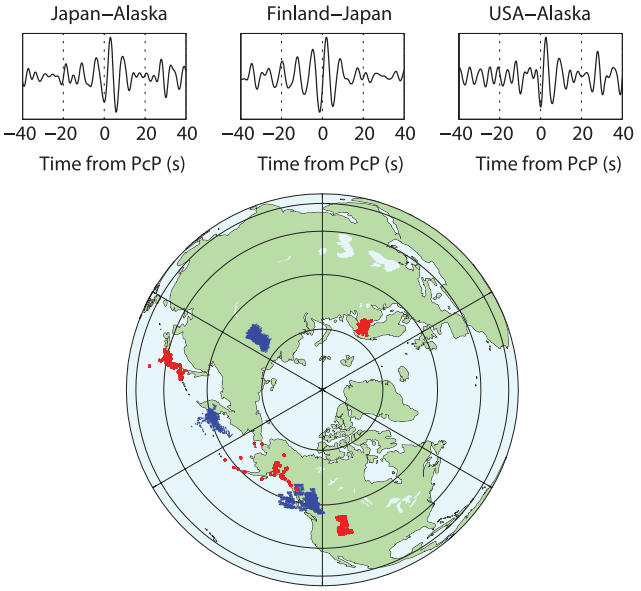

Figure 3. Example of array analysis of PcP seismic waves. The seismic traces are the stacked noise correlations after alignment using PREM. Red dots, stations considered in this analysis; blue dots, surface projections of the reflection points at the core–mantle boundary for each pair of stations.

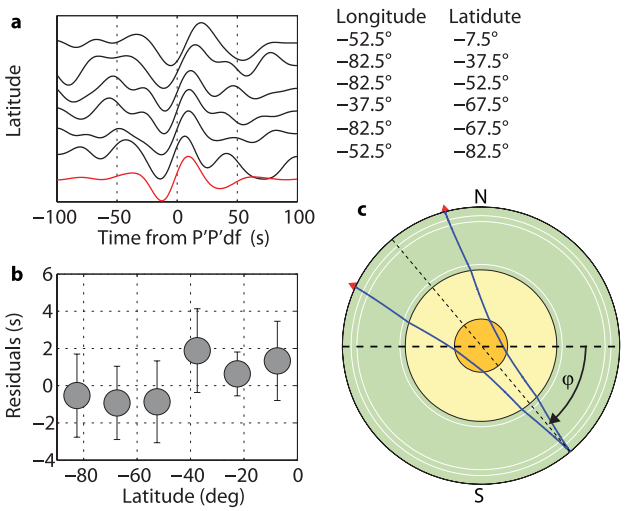

Figure 4. Measurements of core anisotropic propagation. (a) Examples of stacked teleseismic noise correlations with respect to the theoretical arrival times. The reference wavelet used to measure the residual traveltimes is also shown (red). (b) Residual traveltimes for the P′P′df seismic waves as a function of latitude, each obtained as a linear average over all of the bins at a given latitude. Error bars show standard deviations. (c) How the latitude φ is defined.

of the deep Earth. We present here examples that demonstrate that these correlations can be used to study the deep Earth heterogeneity at different depths.

We first tested the feasibility of using these observed *P* waves for lithospheric imaging, as applied to part of the USArray. The stations of the LAPNET array were used as virtual sources, as the array aperture is small and the local lithospheric heterogeneity is very weak (Poli *et al.* 2013). We construct average seismograms between each USArray station and all LAPNET stations. The lithospheric heterogeneity beneath the USArray stations will appear as small time delays between such traces. We estimate these time delays by cross-correlation between each trace and a reference trace, obtained as a stack of all the station specific seismograms. Fig. 2 shows the *P*-wave time delays that we observed across part of the USArray, and compares these with a seismic model of the lithosphere in the same area (Shen *et al.* 2013). The agreement between the model and our observations is striking, and demonstrates that these lithospheric seismic-wave variations can be retrieved using teleseismic noise correlations, such as for the low velocities beneath Yellowstone.

As our correlations showed several waves that sampled the deepest parts of the Earth, we also tested the possibility of using the short-period (5–10 s) PcP waves; that is, *P* waves reflected at the core–mantle boundary (see Fig. 1b). To enhance the small amplitudes of these PcP waves, we also used an array-stacking procedure (Fig. 3). Each trace is the result of the stacking of individual noise correlations between a pair of networks, after traveltime correction according to PREM. PcP waves clearly emerge from the stack with small delays with respect to the average model. The PcP waves arrive earlier on the path between Finland and Japan, in agreement with fast mantle anomalies beneath Russia, whereas larger PcP traveltimes between USA–Alaska and Japan–Alaska agree with the slow velocity mantle structures beneath the Pacific Ocean (Li *et al.* 2008).

Finally, we used the phase P′P′df to analyse the traveltime dependence on latitude; that is, the angle between the travel path and the axis of rotation of the Earth (see Fig. 4c). Seismic observations tend to show that waves propagate faster along polar paths than along equatorial paths, which has lead to the suggestion of inner-core anisotropy (Souriau *et al.* 2003). Testing this hypothesis is however difficult, as very few earthquakes are located at the antipode of seismic receivers, and in particular at high latitudes. We first selected station pairs in the Northern Hemisphere and divided the Southern Hemisphere into a grid of 15° blocks for both latitude and longitude. For each bin, we stacked all of the correlations for which the surface reflection point was contained in the bin. During the stacking, all of the traces were delayed according to PREM and corrected for the Earth ellipticity (Dziewonski & Gilbert 1976). Some examples of these average traces sorted as a function of latitude, are shown in Fig. 4(a). We then measured the time delays between the trace of each bin and the average trace over all of the correlations. Fig. 4(b) shows the average delays (over longitude) for each latitude and their standard deviations. In agreement with earthquake observations, the propagation of the P′P′df waves in noise correlations was slow for equatorial paths as compared to polar paths.

CONCLUSION

Our results show that global teleseismic ambient–noise correlations contain body waves that sample the deep Earth, and these are independent of ballistic waves from earthquakes. In the correlations, it is possible to retrieve the signature of the heterogeneity of the lithosphere, the lateral heterogeneity associated with the waves reflected on the core–mantle boundary and the latitude-dependent delays induced by anisotropy for waves that propagate through the inner core. Teleseismic correlations can therefore provide additional seismograms that complement earthquake data and that contain a wealth of information on the structure of the deep Earth. The development of dense arrays in many regions and modern array processing techniques (Rost & Thomas 2002) make us confident that regions of the

Earth that are at present poorly known can be illuminated in detail through such teleseismic correlations of ambient noise.

ACKNOWLEDGEMENTS

This study was supported by the European Research Council through the advanced grant 'Whisper' 227507. We greatly acknowledge support from the QUEST Initial Training network funded within the EU Marie Curie Program. All of the data used in this study were obtained through the IRIS, NEID and RESIF data centres. We used data from numerous seismic networks, and we thank all of the dedicated seismologists and technical staff who run these networks for making their seismic data available.

REFERENCES

Ardhuin, F., Stutzmann, E., Schimmel, M. & Mangeney, A., 2011. Ocean wave sources of seismic noise, *J. geophys. Res.,* **116,** C09004.

Astiz, L., Earle, P. & Shearer, P., 1996. Global stacking of broadband seismograms, *Seism. Res. Lett.,* **67,** 8–18.

Campillo, M. & Paul, A., 2003. Long-range correlations in the seismic coda, *Science,* **299,** 547–549.

Dziewonski, A.M. & Gilbert, F., 1976. The effect of small aspherical perturbations on travel times and a re-examination of the corrections for ellipticity, *Geophys. J. R. astr. Soc.,* **44,** 7–17.

Dziewonski, A.M. & Anderson, D.L., 1981. Preliminary reference Earth model, *Phys. Earth planet. Inter.,* **25,** 297–356.

Fukao, Y.K., Nishida, K. & Kobayashi, N., 2010. Seafloor topography, ocean infragravity waves, and background Love and Rayleigh waves, *J. geophys. Res.,* **115,** B04302.

Gerstoft, P., Shearer, P.M., Harmon, N. & Zhang, J., 2008. Global P, PP, and PKP wave microseisms observed from distant storms, *Geophys. Res. Lett.,* **35,** L23307.

Hillers, G., Graham, N., Campillo, M., Kedar, S., Landès, M. & Shapiro, N., 2012. Global oceanic microseism sources as seen by seismic arrays and predicted by wave action models, *Geochem. Geophys. Geosyst.,* **13,** Q01021.

Kurrle, D. & Widmer-Schnidrig, R., 2008. The horizontal hum of the Earth: a global background of spheroidal and toroidal modes, *Geophys. Res. Lett.,* **35,** L06304.

Landès, M., Hubans, F., Shapiro, N.M., Paul, A. & Campillo, M., 2010. Origin of deep ocean microseisms by using teleseismic body waves, *J. geophys. Res.,* **115,** B05302.

Li, C., van der Hilst, R.D., Engdahl, E.R. & Burdick, S., 2008. A new global model for P wave speed variations in Earth's mantle, *Geochem. Geophys. Geosyst.,* **9,** Q05018.

Lin, F.C., Tsai, V.C., Schmandt, B., Duputel, Z. & Zhan, Z., 2013. Extracting seismic core phases with array interferometry, *Geophys. Res. Lett.,* **40**(6), 1049–1053.

Longuet-Higgins, M.S., 1950. A theory of the origin of microseisms, *Phil. Trans. R. Soc. Lond., A.,* **243,** 1–35.

Nishida, K., Kawakatsu, H., Fukao, Y. & Obara, K., 2008. Background Love and Rayleigh waves simultaneously generated at the Pacific Ocean floors, *Geophys. Res. Lett.,* **35,** L16307.

Nishida, K., 2013. Global propagation of body waves revealed by cross-correlation analysis of seismic hum, *J. geophys. Res.,* in press, doi:10.1002/grl.50269.

Nissen-Meyer, T., Fournier, A. & Dahlen, F.A., 2007. A 2-D spectral-element method for computing spherical-earth seismograms–I. Moment-tensor source, *Geophys. J. Int.,* **168**(3), 1067–1093.

Nissen-Meyer, T., Fournier, A. & Dahlen, F.A., 2008. A 2-D spectral-element method for computing spherical-earth seismograms–II. Waves in solid-fluid media, *Geophys. J. Int.,* **174**(3), 873–888.

Poli, P., Pedersen, H.A., Campillo, M. & the POLENET/LAPNET Working Group, 2012a. Emergence of body waves from cross-correlation of short period seismic noise, *Geophys. J. Int.,* **188,** 549–558.

Poli, P., Campillo, M., Pedersen, H. & the Lapnet Working Group, 2012b. Body wave imaging of the Earth's mantle discontinuities from ambient seismic noise, *Science,* **338,** 1063–1065.

Poli, P., Pedersen, H.A., Campillo, M. & the POLENET/LAPNET Working Group, 2013. Noise directivity and group velocity tomography in a region with small velocity contrasts: the northern Baltic Shield, *Geophys. J. Int.,* **192,** 413–424.

Rost, S. & Thomas, C., 2002. Array seismology: methods and applications, *Rev. Geophys.,* **40**(3), 1008.

Ruigrok, E., Campman, X. & Wapenaar, K., 2011. Extraction of P-wave reflections from microseisms, *C. R. Geosci.,* **343,** 512–525.

Sabra, K.G., Roux, P. & Kuperman, W.A., 2004. Arrival-time structure of the time-averaged ambient noise cross-correlation function in an oceanic waveguide, *J. acoust. Soc. Am.,* **117**(1), 164–174.

Sánchez-Sesma, F.J. & Campillo, M., 2006. Retrieval of the Green function from cross-correlation: the canonical elastic problem, *Bull. seism. Soc. Am.,* **96,** 1182–1191.

Shapiro, N.M. & Campillo, M., 2004. Emergence of broadband Rayleigh waves from correlations of the seismic ambient noise, *Geophys. Res. Lett.,* **31,** L07614.

Shen, W., Ritzwoller, M.H. & Schulte-Pelkum, V., 2013. A 3-D model of the crust and uppermost mantle beneath the central and western US by joint inversion of receiver functions and surface wave dispersion, *J. geophys. Res.,* **118,** 1–15.

Souriau, A., Garcia, R. & Poupinet, G., 2003. The seismological picture of the inner core: structure and rotation, *C. R. Geoscience,* **335,** 51–63.

Vinnik, L.P., 1973. Sources of microseismic P waves, *Pure appl. Geophys.,* **103**(1), 282–289.

Zhan, Z., Ni, S., Helmberger, D.V. & Clayton, R.W., 2010. Retrieval of moho reflected shear wave arrivals from ambient seismic noise, *Geophys. J. Int.,* **1,** 408–420.

Shapiro, N.M., Ritzwoller, M.H. & Bensen, G.D., 2006. Source location of the 26 sec microseism from cross correlations of ambient seismic noise, *Geophys. Res. Lett.,* **33,** L18310.

Bensen, G.D., Ritzwoller, M.H., Barmin, M.P., Levshin, A.L., Lin, F., Moschetti, M.P., Shapiro, N.M. & Yang, Y., 2007. Processing seismic ambient noise data to obtain reliable broad-band surface wave dispersion measurements, *Geophys. J. Int.,* **169,** 1239–1260.

SUPPORTING INFORMATION

Additional Supporting Information may be found in the online version of this article:

Figure S1. Teleseismic correlation section. The traveltime curves for the PREM model are represented as red dots. In supplement to P,PP, PKP, P′P′df and ScS shown in Fig. 1, other late phases are also visible without further processing such as PKPPKS, PKPPcP, PKIKP, S, SS, SSS, ScS, SKP, SKKP or PcPPKSPKS.

Figure S2. Raw teleseismic correlations in the 5–10 s period band between Finland and central USA, showing (a) P and PcP and (b) and P′P′ df.

Figure S3. Positive and negative time correlations between LapNet (Finland) and FNet (Japan) showing for P and PcP phases. The waves propagating from Finland to Japan or from Japan to Finland exhibit similar amplitude and signal-to-noise ratio.

APPENDIX. (http://gji.oxfordjournals.org/lookup/suppl/doi:10.1093/gji/ggt160/-/DC1)

Please note: Oxford University Press are not responsible for the content or functionality of any supporting materials supplied by the authors. Any queries (other than missing material) should be directed to the corresponding author for the article.